INTERNATIONAL JOURNAL OF REFRIGERATION 33 (2010) 1478–1488

available at www.sciencedirect.com

ScienceDirect

journal homepage: www.elsevier.com/locate/ijrefrig

Reduction of the refrigerant-induced noise from the evaporator-inlet pipe in a refrigerator

Hyung Suk Han [a], *Weui Bong Jeong* [b,*], *Min Seong Kim* [b], *Soo Young Lee* [c], *Min Young Seo* [d]

[a] *1st Team, Naval Sea System Center, Defense Agency for Technology and Quality, 1, Aju-dong, Geoje, South Korea*
[b] *Department of Mechanical Engineering, Pusan National University, Jangjeon-dong, Kumjung-ku, Pusan, Republic of Korea*
[c] *Department of Mechanical Engineering, SunkyunKwan University, Cheoncheon-dong, Suwon, South Korea*
[d] *Engineering Design Department, LG Electronics, Gaeumjeong-dong, Changwon, South Korea*

ARTICLE INFO

Article history:
Received 15 December 2009
Received in revised form
1 May 2010
Accepted 22 May 2010
Available online 2 June 2010

Keywords:
Refrigerator
Evaporator
Review
Reduction
Noise
Refrigerant
Correlation
Two-phase flow
Bubble

ABSTRACT

The flow pattern of the refrigerant in an evaporator-inlet pipe is a very important factor for determining the type of refrigerant-induced noise because the shape and size of the bubble are different according to the flow pattern in the pipe. In this study, the relations between refrigerant-induced noise and flow patterns are discussed. The flow patterns of the fluid in horizontal and vertical pipes were also estimated using Hewitt, Taitel–Dukler and Oshinowo–Charles maps. The refrigerant-supplying equipment was used to monitor the characteristics of the flow in the experiments. The shape and layout of evaporator-inlet pipe were suggested not to be the intermittent flow pattern. The noise level radiated from the refrigerator could be reduced by about 2–5 dB in the frequency range from 315 Hz to 3.15 kHz.

Diminution du bruit engendré par le frigorigène dans la conduite d'entrée de l'évaporateur

Mots clés : Réfrigérateur ; Évaporateur ; Synthése ; Réduction ; Bruit ; Frigorigène ; Corrélation ; Écoulement diphasique ; Bulle

* *Corresponding author*. Tel.: +82 51 510 2337; fax: +82 51 517 3805.
E-mail address: wbjeong@pusan.ac.kr (W.B. Jeong).

doi:10.1016/j.ijrefrig.2010.05.014

Nomenclature

A	Sectional area of the pipe [m^2]
b	Radiation resistance of the bubble [N s m^{-1}]
d	Diameter of the pipe [m]
f_n	Natural frequency of oscillating bubble [Hz]
Fr	Froude number
g	Acceleration of gravity [m s^{-2}]
G_l	Mass flux of the liquid [kg m^{-2} s^{-1}]
G_g	Mass flux of the gas [kg m^{-2} s^{-1}]
h	Convection coefficient [kJ m^{-2}°C^{-1}]
h'	Enthalpy of the refrigerant at an evaporator-inlet [kJ kg^{-1}]
h_f	Enthalpy of the saturated liquid at low pressure [kJ kg^{-1}]
h_g	Enthalpy of the saturated gas at low pressure [kJ kg^{-1}]
h_{sc}	Enthalpy of the sub-cooler [kJ kg^{-1}]
k	Equivalent stiffness term of the bubble [N m^{-1}]
K	Conductivity of the insulation [kJ m^{-1}°C^{-1}]
Ku_g	Kutateladze parameter of the gas
j	Superficial velocity [m s^{-1}]
j_g	Superficial velocity of the gas [m s^{-1}]
j_l	Superficial velocity of the liquid [m s^{-1}]
l	Length of the pipe[m]
L	Length of the long bubble [m]
m	Equivalent mass of the bubble [kg]
m'	Mass flow rate [kg s^{-1}]
p	Pressure of the liquid surrounding of the bubble [Pa]
P_A	Acoustic pressure of the bubble [Pa]
Q	Total volumetric flow rate [m^3 s^{-1}]
Q_g	Volumetric flow rate of the gas [m^3 s^{-1}]
Q_l	Volumetric flow rate of the liquid [m^3 s^{-1}]
q_{heater}	Heat input from the heater to the operating refrigerant [kJ]
q_{pipe}	Heat transferred from the connection pipe to the environment[kJ]
r_{pipe}	Radius of the pipe [m]
r_{insul}	Radius of the insulation [m]
R_0	Equivalent radius of the bubble assuming its shape is spherical [m]
R	Inner radius of the pipe [m]
t	Time [s]
T	Period of oscillation [s]
T_∞	Environmental temperature [°C]
T_{pipe}	Temperature on the pipe [°C]
v	Volume of the bubble [m^3]
V_0	Initial volume of the bubble [m^3]
x	Vapor quality
X	the Martinelli parameter
α	Amplitude of oscillation
β	Volumetric quality
γ	specific heat ratio
Δh_{heater}	Enthalpy increment by the heater [kJ kg^{-1}]
Δh_{pipe}	Enthalpy increment by heat exchanging from the connecting pipe to the environment [kJ kg^{-1}]
κ	polytropic index
μ	Viscosity [N s m^{-2}]
μl	Viscosity of the liquid [N s m]$^{-2}$]
μ_{water}	Viscosity of the water [N s m^{-2}]
ρ	Density of the liquid surrounding of the bubble [kg m^{-3}]
ρ_l	Density of the liquid [kg m^{-3}]
ρ_g	Density of the gas [kg m^{-3}]
ρ_{water}	Density of the water [kg m^{-3}]
ρ_{air}	Density of the air [kg m^{-3}]
σ	Surface tension [N m^{-1}]
σ_{water}	Surface tension of the water [N m^{-1}]
ω	Radius frequency
$[dp/dz]_g$	Frictional pressure gradient assuming that the gas flows alone in a tube [Pa m^{-1}]
$[dp/dz]_l$	Frictional pressure gradient assuming that the liquid flows alone in a tube [Pa m^{-1}]

1. Introduction

Reducing the refrigerant-induced noise of the refrigerator is one of the many problems that have to be solved in the development of a refrigerator. The solution to this problem demands much cost and manpower. Since noises from home appliances other than the refrigerator have been diminishing these days, the refrigerant-induced noise from the refrigerator can be heard more easily than before. Therefore, customers are seeking reduction of such noise from refrigerators.

Refrigerant-induced noise usually occurs when the refrigerant is in 2-phase state. Since the characteristics of the fluid dynamics of 2-phase flows vary with the characteristics of the gas bubble, the gas bubble is considered to be one of the main sources of noise in 2-phase flow. The acoustic characteristics of a gas bubble were firstly researched by Minnaert (1933). Minnaert found the sound of a rising bubble radiated from the nozzle is related to the natural frequency of it. This relationship is generally expressed by the Minnaert equation. Strasberg (1956) found that a bubble that varies its volume radiated sound. Since the characteristics of a gas bubble such as the shape and size are different according to the flow pattern in a pipe, it can be estimated that the flow pattern is strongly related to the refrigerant-induced noise. Flow pattern has been studied usually by experiments. Representative studies on the flow pattern of a horizontal flow are those of Baker (1954), Mandhane et al. (1974), Hashizume (1983), Taitel and Dukler (1976) and Thome and Hajal (2003). And the flow pattern of a vertical flow has been studied by Hewitt and Roberts (1969), Oshinowo and Charles (1974) and Taitel and Dukler (1977). Taitel and Dukler were the first to study the transition of the flow pattern by theoretical approach.

The acoustics of bubbles in a pipe has been also studied by experiments. Oguz and Prosperetti (1998) researched the acoustic characteristics of bubbles in a pipe. Since the large bubble in a pipe is constrained with the wall of the pipe, the resonance frequency should be different compared to that of the freely rising bubble. They investigated the resonance frequencies of the bubbles in a pipe experimentally and compared them to those of freely rising bubbles. Han et al. (2009) studied the root causes of the refrigerant-induced noise experimentally. They found that the refrigerant-induced noise was strongly related to the flow pattern in a pipe. They experimentally verified that the acoustic noise was increased when the flow pattern in a pipe was intermittent flow. However, the researches about the acoustic characteristics of a 2-phase flow considering both flow pattern and bubble dynamics simultaneously haven't been performed widely.

However, the research about the acoustic characteristics of a 2-phase refrigerant flow considering both flow pattern and bubble dynamics simultaneously has been rarely performed.

In this research, the refrigerant-induced noise from the evaporator-inlet pipe in a refrigerator is studied considering the flow pattern and the bubble dynamics in the pipe experimentally. In order to investigate the refrigerant-induced noise more objectively in the experiment, a system for evaluating the refrigerant-induced noise was developed. Through the evaluation system and associated theories about refrigerant-induced noise, the evaporator-inlet pipe, where the refrigerant-induced noise is most serious in a refrigerator, is redesigned and evaluated to reduce the refrigerant-induced noise. And also the relationship between the flow pattern in a pipe and the refrigerant-induced noise is verified by applying redesigned evaporator-inlet pipe to the real refrigerator.

2. Test setup

In order to evaluate the noise of the refrigerator according to the different conditions of the evaporator-inlet pipe, an evaluation system of the refrigerant-induced noise was developed, as shown in Fig. 1. The capacities of the components of the evaluation system are shown in Table 1.

The refrigerant-supplying equipment is connected to the test unit in the anechoic chamber (size: W2.5 m × D2.0 m × H2.1 m). This connection allows the simultaneous measurement of noise as well as cycle temperature. The refrigerant supplying equipment can be controlled to maintain the typical cycle condition that gives serious refrigerant-induced noise. The test unit in the anechoic chamber only consists of the evaporator and the fan, therefore, the noise from the evaporator at a typical cyclic condition can be measured according to the variation of the evaporator-inlet pipe condition, assuming that the fan noise is constant for different cycle conditions. The refrigerant to be tested in this equipment was R600a. The linear compressor supplies it to the refrigerant-supplying equipment. As the refrigerant flows through the condenser, its pressure is controlled by the amount of the heat-exchange between the condenser and the second cyclic line of R12 refrigerant. A sub-cooler, linked with the condenser, controls the sub-cooling degree of the refrigerant. The sub-cooled refrigerant is expanded by an electric expansion valve (Paker SEI-05) and then it enters the heater, which controls the vapor quality of the expanded refrigerant. The vapor quality can be calculated from the enthalpy of the refrigerant at the heater-outlet as given in Eqs. (1)–(3).

$$x = \frac{h' - h_f}{h_g - h_f} \tag{1}$$

$$h' = h_{sc} + \Delta h_{heater} + \Delta h_{pipe},\ where\ \Delta h_{heater} = \frac{q_{heater}}{m'},\ \Delta h_{pipe} = \frac{q_{pipe}}{m'} \tag{2}$$

$$q_{pipe} = \frac{(T_\infty - T_{pipe})}{R_1 + R_2},\ where\ R_1 = \frac{1}{2\pi Kl}\ln\left(\frac{r_{insul}}{r_{pipe}}\right),\ R_2 = \frac{1}{h(2\pi r_{insul} l)} \tag{3}$$

When the refrigerant passes through the heater, the enthalpy is increased by the heater. The enthalpy will also

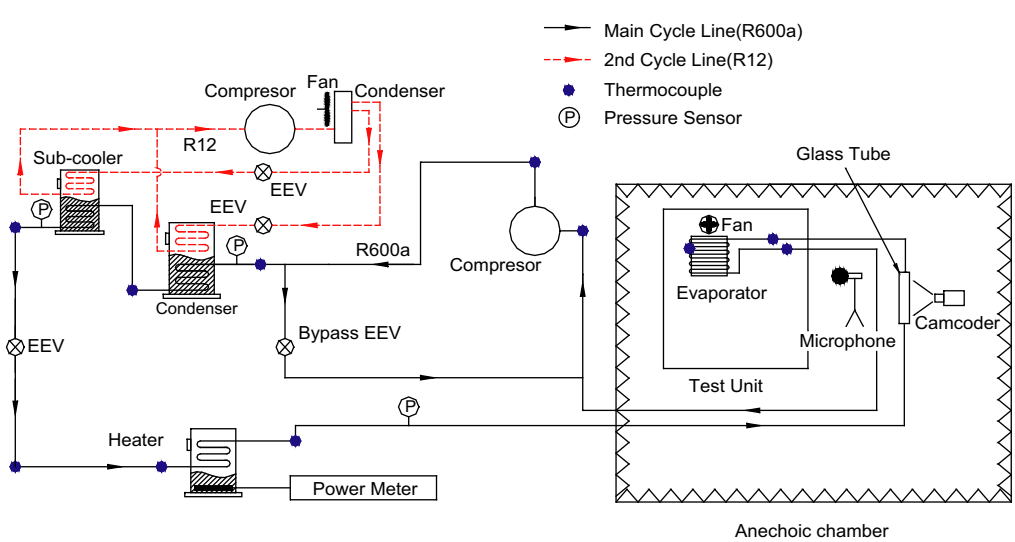

Fig. 1 – Evaluation equipment for refrigerant-induced noise.

Table 1 – Capacities of the components of the refrigerant-supplying equipment.

Component	Capacity	Maker
Compressor	0.3 kW	LG, Korea
Condenser	0.72 kW	Hwashin, Korea
Sub-cooler	0.72 kW	Hwashin, Korea
Heater	0.6 kW	Hwashin, Korea

vary when the refrigerant goes through the pipe from the outlet of an expansion valve to the inlet of an evaporator because of the heat exchanging to the environment. Hence, this heat exchanging should be considered calculating the enthalpy.

In order to monitor the thermodynamic cyclic condition (including p–h diagram), high and low pressure of the refrigerant cycle were measured by pressure sensor and the temperature of the discharge, suction, condenser, sub-cooler, expansion valve, heater and evaporator were measured by T-type thermocouples. All of the cyclic data were collected by the data logger (Agilent 34970A).

A sight glass was installed at the evaporator-inlet pipe of the test unit as shown in Fig. 2a to visualize the flow pattern with a digital camcorder. A microphone (B&K Type 4189) was installed at the rear side of the test unit, where the refrigerant-induced noise occurred most seriously as shown in Fig. 2b. With this setup, the flow pattern in the evaporator-inlet pipe of the test unit could be controlled, and the noise of the test unit could be measured simultaneously according to the flow pattern.

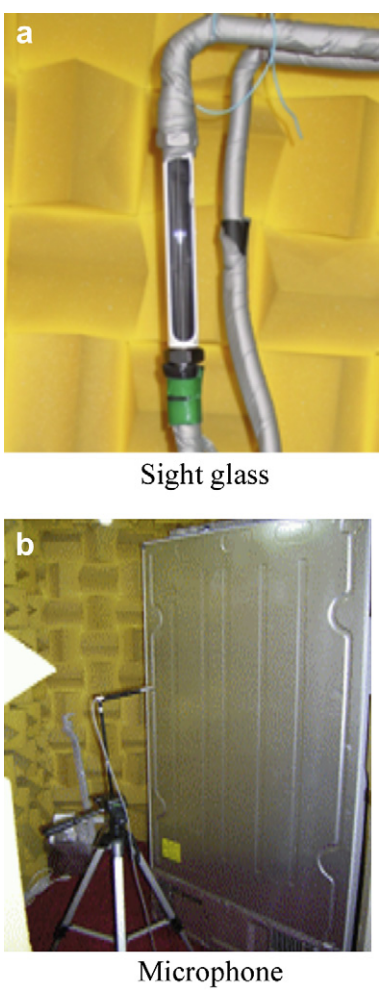

Fig. 2 – Test setup.

In the measured noise data, there will be some other noise unrelated to the flow patterns of the refrigerant, such as the noises due to the cyclic variations. In this research, however, it is assumed that the variation of the noise occurs only by the variation of the flow patterns. There are also uncertainties about the flow patterns since judging the flow patterns from the visualization of the flow passing through sight glass is subjective method.

3. Noise characteristics of evaporator-inlet pipe

The size and shape of bubbles are different according to the flow pattern in a pipe. Therefore, the acoustic characteristics should vary according to the flow pattern in the pipe. The acoustic characteristics can be estimated by Eq. (4) (Strasberg, 1956) assuming that a unit bubble can be modeled as a one degree-of-freedom spring-mass system.

$$m\ddot{v} + b\dot{v} + k(v - V_0) = P_A e^{j\omega t} \tag{4}$$

where,

$$m = \frac{\rho}{4\pi R_0}, \quad k = \frac{\gamma p}{V_0}$$

Let us assume that the volume of a bubble oscillates with amplitude of α, as given in Eq. (5).

$$v = V_0 + \alpha \sin\frac{2\pi t}{T} \tag{5}$$

Then, the natural frequency f_n of the oscillating bubble can be given as Eq. (6) (Minnaert, 1933).

$$f_n = \frac{1}{2\pi R_0}\sqrt{\frac{3kp}{\rho}} \tag{6}$$

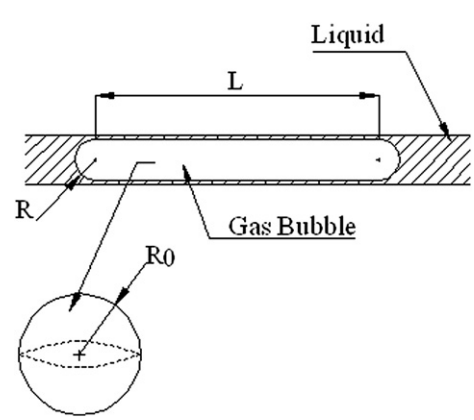

Fig. 3 – Shape of the bubble with larger equivalent radius than tube radius (R_0:Equivalent radius).

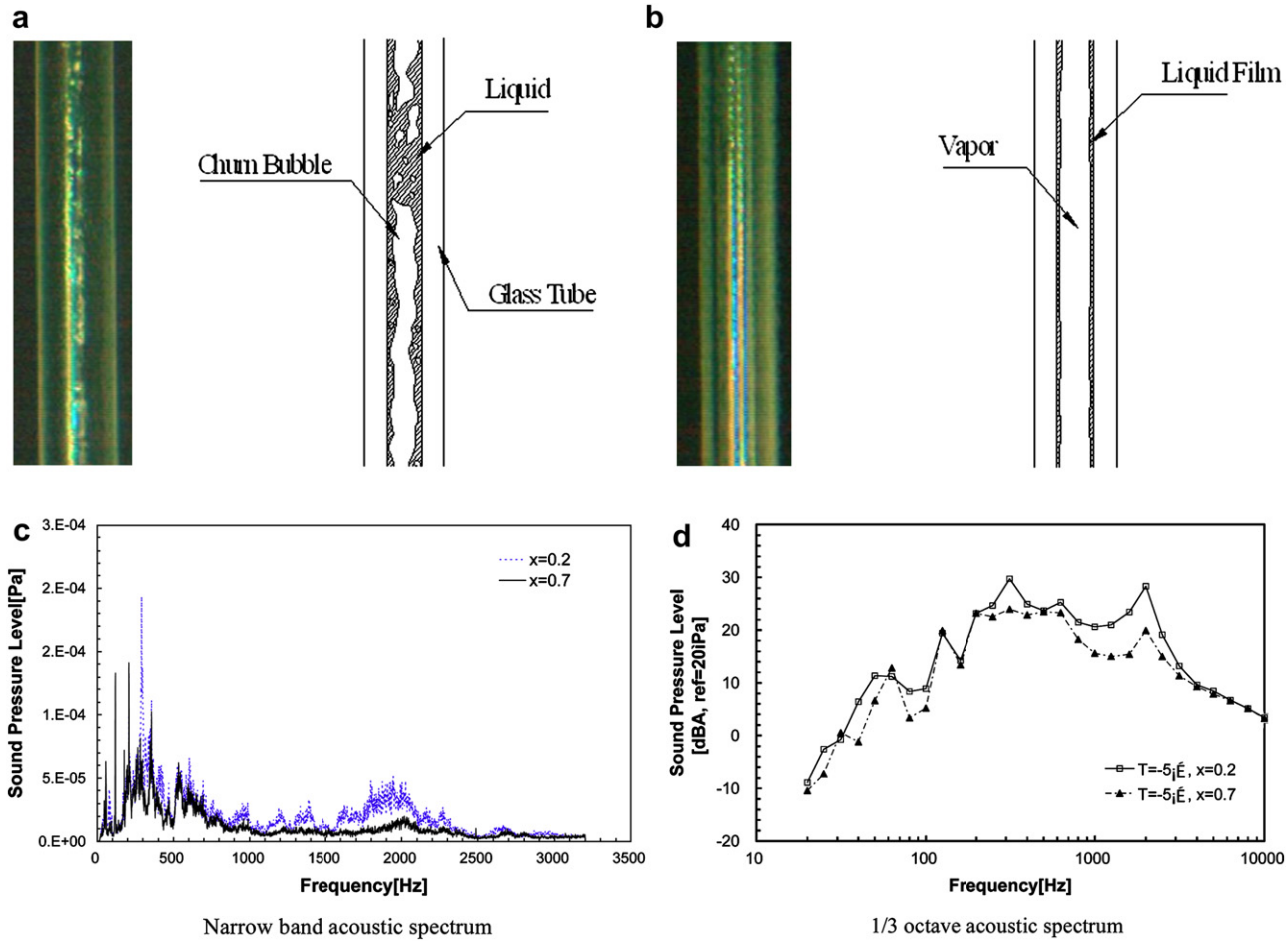

Fig. 4 – Flow patterns and their acoustic spectra.

The bubble shape cannot be spherical when the equivalent radius of the bubble is larger than the radius of the inner pipe. Because the radius of bubble is larger than the radius of the pipe, it should be deformed irregularly with axial direction of the pipe. The shape of the slug flow is a well-known bullet shape. In this study, a long bullet shape is assumed to be cylindrical shape as shown in Fig. 3 in order to explain its frequency characteristics easily.

Consequently, low-frequency noise occurs from the bubble in the intermittent flow, whose equivalent radius is longer than the radius of the pipe. The theoretical review in this section showed that refrigerant-induced noise is strongly related to the flow pattern in a pipe.

In order to validate these theoretical estimations of the acoustic characteristics, noise was measured with the evaluation system when the flow pattern of the evaporator-inlet pipe in the test unit was churn flow and annular flow, respectively. Here, the test condition was as follows: the mass flow rate was 2.77 kg/h ± 1%, the temperature was −5 °C ± 1 °C at the evaporator-inlet pipe and the inner diameter of the pipe was 4.35 mm. The sub-cooling degree and vapor quality of the commercial refrigerator are about 15 °C and 0.3 respectively. However, in this research, the variation of the acoustic noise was monitored as the vapor quality changes from very low level (about 0.1–0.2) to high level (about 0.7). The sub-cooling degree of the refrigerant-supplying equipment was set to 30 °C in order to reduce the vapor quality until 0.1–0.2 at the evaporator-inlet. The flow pattern of the refrigerant at the evaporator-inlet pipe can be transitioned by increasing the vapor quality with the heater installed in the refrigerant-supplying equipment, as shown in Fig. 1. In order to reduce the effect of the cyclic variation on the noise in this test, the high and low pressure as well as sub-cooling degree were controlled to be constant (high pressure = 0.68 Mpa ± 2%, low pressure = 0.13 Mpa ± 2%, sub-cooling degree = 30 °C ± 1 °C) when the heater was controlled.

Fig. 4a shows that the flow pattern becomes churn flow when the vapor quality is 0.2 and Fig. 4b shows that the flow pattern transitioned to annular flow when the vapor quality reaches 0.7. Here, the vapor quality is calculated with the enthalpy at the evaporator-inlet as given in Eqs. (1)–(3) as given in the previous section.

Fig. 4c and d shows narrow-band and 1/3 octave acoustic spectra at these two conditions respectively. Fig. 4c shows that the acoustic characteristics between the churn and annular flow are completely different, as referred in the previous section. In Fig. 4d, it can be known that the noises at 315 Hz and 2.0 kHz were reduced by about 3.0 dB (50% of the original sound pressure) and 4.5 dB (35% of the original sound pressure) respectively when the flow pattern in the pipe

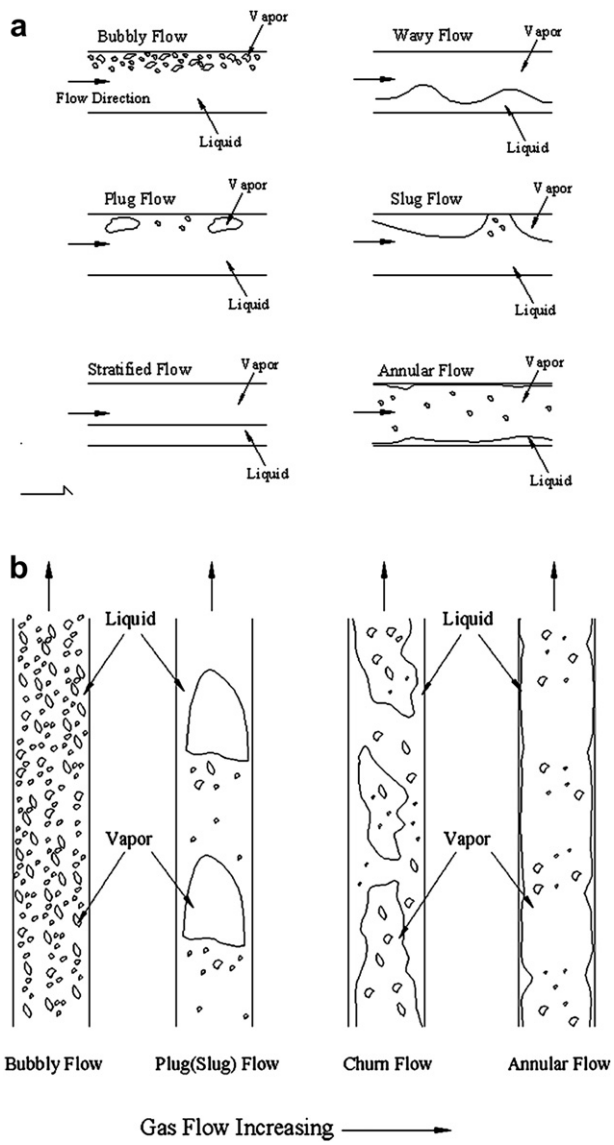

Fig. 5 – Schematic diagram of the flow patterns.

transitioned from churn to the annular flow. Considering Minnaert equation given in Eq. (6), the equivalent radius of the bubble in the pipe can be calculated, assuming that the noises at 315 Hz and 2 kHz were due to the resonance of the bubbles. For the given cyclic condition ($T = -5\,^{\circ}C \pm 1\,^{\circ}C$), the equivalent radius is 13.9 mm for 315 Hz and is 2.18 mm for 2 kHz. The equivalent radius of the bubble having resonance frequency of 315 Hz should be longer than the radius of the pipe ($r = 2.175$ mm). Therefore, the noise at 315 Hz should be caused by the bubble having a long cylindrical shape such as bubbles in the slug and churn flow. However, the equivalent radius of the bubble having the resonance frequency of 2 kHz is almost equal to the radius of the evaporator-inlet pipe. Therefore, the bubbles resonating at 2 kHz correspond to the churn flow pattern because a churn bubble is usually accompanied by small bubbles due to its highly oscillating characteristics.

These test results and frequency analysis verify that refrigerant-induced noise increases when the flow pattern in a pipe is intermittent flow such as churn flow.

4. Estimation of flow patterns

The previous section explains that refrigerant-induced noise is strongly related to the flow pattern in a pipe. Because of gravity, flow patterns vary along the flow direction. Therefore, the flow patterns are usually classified by the type of pipe, either horizontal or vertical. The flow pattern in a horizontal pipe can be classified according to the shape of the flow such as bubbly-, plug-, stratified-, wavy-, slug- and annular flow and those in the vertical pipe can be classified to bubbly-.slug-, churn- and annular flow, as shown in Fig. 5.

The flow patterns in a horizontal or vertical pipe have different characteristics even in the same cyclic condition. Therefore, in this section, the flow patterns are estimated with various flow pattern maps for the refrigerant at the evaporator-inlet pipe for the commercial cyclic conditions of the refrigerator.

It is widely known that the length of the pipe should be longer than 40 times of the diameter so that the refrigerant has fully developed flow pattern in a pipe. The pipe between expansion-valve and the evaporator-inlet was designed with length of 2 m so that the refrigerant can be fully developed. Therefore, in this research, the flow pattern in an evaporator-inlet pipe of the commercial refrigerator can be assumed to be one of the typical flow patterns shown in Fig. 5.

In order to estimate whether the refrigerant-induced noise occurs or not at given flow pattern, the characteristics of the sound of each flow pattern should be defined preliminarily. Considering the characteristics of the sound for the bubbles in

Table 2 – Flow pattern map for the horizontal flow.

Flow pattern Map	Map coordinate	
	X	Y
Baker (1954)	$G_l\,\psi$ where $G_l = \frac{m'(1-x)}{A}$, $\psi = \frac{\sigma_{water}}{\sigma}\left(\frac{\mu_l}{\mu_{water}}\cdot\frac{\rho_{water}}{\rho_l}\right)^{1/3}$	G_g/λ where $G_g = \frac{m'x}{A}$, $\lambda = \left(\frac{\rho_g}{\rho_{air}}\cdot\frac{\rho_l}{\rho_{water}}\right)^{1/2}$
Hashizume (1983)	$G_l\,\psi$ where $G_l = \frac{m'(1-x)}{A}$, $\psi = \left(\frac{\sigma_{water}}{\sigma}\right)^{1/4}\left(\frac{\mu_l}{\mu_{water}}\cdot\frac{\rho_{water}}{\rho_l}\right)^{1/3}$	G_g/λ where $G_g = \frac{m'x}{A}$, $\lambda = \left(\frac{\rho_g}{\rho_{air}}\cdot\frac{\rho_l}{\rho_{water}}\right)^{1/2}$
Mandhane et al. (1974)	$j_l = \frac{Q_l}{A} = \frac{G_l}{\rho_l}$	$j_g = \frac{Q_g}{A} = \frac{G_g}{\rho_g}$
Taitel and Dukler (1976)	$X = \frac{(dp/dz)_l}{(dp/dz)_g} = \left(\frac{1-x}{x}\right)^{0.875}\left(\frac{\rho_g}{\rho_l}\right)^{0.5}\left(\frac{\mu_l}{\mu_g}\right)^{0.125}$	$Fr = \frac{G_g}{[\rho_g(\rho_l-\rho_g)\cdot d\cdot g]^{1/2}}$
Thome and Hajal (2003)	m'	x

Table 3 – Flow pattern map for the vertical flow.

Flow pattern map	Map coordinate	
	X	Y
Hewitt and Roberts (1969)	G_l^2/ρ_l	G_g^2/ρ_g
Oshinowo and Charles (1974)	$[\beta(1-\beta)]^{-1/2}$ where $\beta = \frac{Q_g}{Q}$	$Fr \cdot \Lambda^{1/2}$ where $Fr = \frac{j^2}{gd}$, $\Lambda = \frac{\mu_l}{\mu_g}[\frac{\rho_l}{\rho_g}(\frac{\sigma}{\sigma_{water}})^3]^{-1/4}$
Taitel and Dukler (1977)	$X = \frac{(dp/dz)_l}{(dp/dz)_g} = (\frac{1-x}{x})^{0.875}(\frac{\rho_g}{\rho_l})^{0.5}(\frac{\mu_l}{\mu_g})^{0.125}$	$Ku_g = j_g\rho_g/[g(\rho_l-\rho_g)\sigma]^{1/4}$

2-phase fluid, the acoustic properties of the each flow pattern can be described as follows;

(1) Bubbly flow
In bubbly flow, there are many small bubbles with spherical shape. The noise may have some tonal sound in accordance with their resonance frequencies. Considering Eq. (6) in the previous chapter, it can be estimated that the frequency of the bubble is high because of the small radius of bubbles in the bubbly flow.

(2) Wavy/Stratified flow
When the flow pattern in a pipe is wavy or stratified, the liquid and gas is divided exactly and there is little bubble in the liquid. The sound level is not dominantly related to the gas bubble but to the velocity of the fluid. It can be estimated that the wavy and stratified flow don't produce much sound (Diatschenco et al., 1994).

(3) Intermittent (slug or churn) flow
The length of the slug and churn bubble is usually long. When the slug flow transitions to churn flow, its volume oscillates severely which causes big noise. The frequency of the oscillating bubble is low because of its large equivalent radius.

(4) Annular flow
When the flow pattern is annular, the liquid flows along the pipe wall and the gas flows at the center core of the pipe. There is little bubble in the annular flow. The flow has relatively high velocity due to its high vapor quality. The sound has broad band frequencies with wide range of the higher frequency and with no typical tonal sound.

Tables 2 and 3 present the parameters of the various flow pattern maps quoted in this research. Table 4 shows the flow patterns in the vertical and the horizontal pipe estimated from various flow pattern maps, as given in Tables 2 and 3. In the estimation, the inner diameter of the evaporator inlet pipe is 4.35 mm and mass flow rate is 2.77 kg/h ± 1%. In Table 4, the flow pattern in the horizontal pipe is estimated to be wavy or annular flow at the operating cyclic range of the refrigerator. Since those flow patterns for the horizontal pipe are good ones with respect to the noise as discussed above, it is estimated that the horizontal pipe has low refrigerant-induced noise. However, the flow pattern in the vertical pipe is estimated to be intermittent (slug or churn) flow at the low mass quality range. It means that the refrigerant induced noise may increase at this condition for the vertical pipe due to the acoustic property of the intermittent flow. Therefore, the horizontal layout of the pipe would be better than vertical one considering the estimated flow patterns at the operating cyclic range of the refrigerator as well as their acoustic properties.

5. Redesign of evaporator inlet pipe to reduce refrigerant-induce noise

Based on the previous section, a horizontal layout of the pipe is more suitable than a vertical one to reduce the refrigerant-induced noise. But it is impossible to make an evaporator-inlet pipe with only horizontal pipes. Therefore, the mitigation of intermittent flow in the vertical pipe will be discussed.

Table 4 – Estimation of the flow patterns at the horizontal and vertical evaporator-inlet pipe for the operating cycle of the commercial refrigerator.

Operating time from start (min)		4	8	12	20	30	60	100
Temperature (°C)		−10.3	−11.3	−12.5	−14.6	−16.4	−19.5	−28.7
Pressure (Mpa)		0.1066	0.1026	0.09783	0.08995	0.08354	0.07361	0.04908
Vapor quality		0.28	0.31	0.33	0.34	0.36	0.38	0.41
Flow direction	Kind of flow pattern map	Estimated flow pattern						
Horizontal flow	Baker map	A	A	A	A	A	A	A
	Hashizume map	W	W	W	W	A	A	A
	Mandhane map	W	W	W	W	W	W	A
	Taitel–Dukler map	A	A	A	A	A	A	A
	Thome–Hajal	W	W	W	W	W	W	W
Vertical flow	Hewitt map	C	C	C	C	C	C	
	Oshinowo–Charles map	C	A	A	A	A	A	A
	Taitel–Dukler map	S/C	A	A	A	A	A	A

A: Annular, C: Churn, S: Slug, W: Wavy.

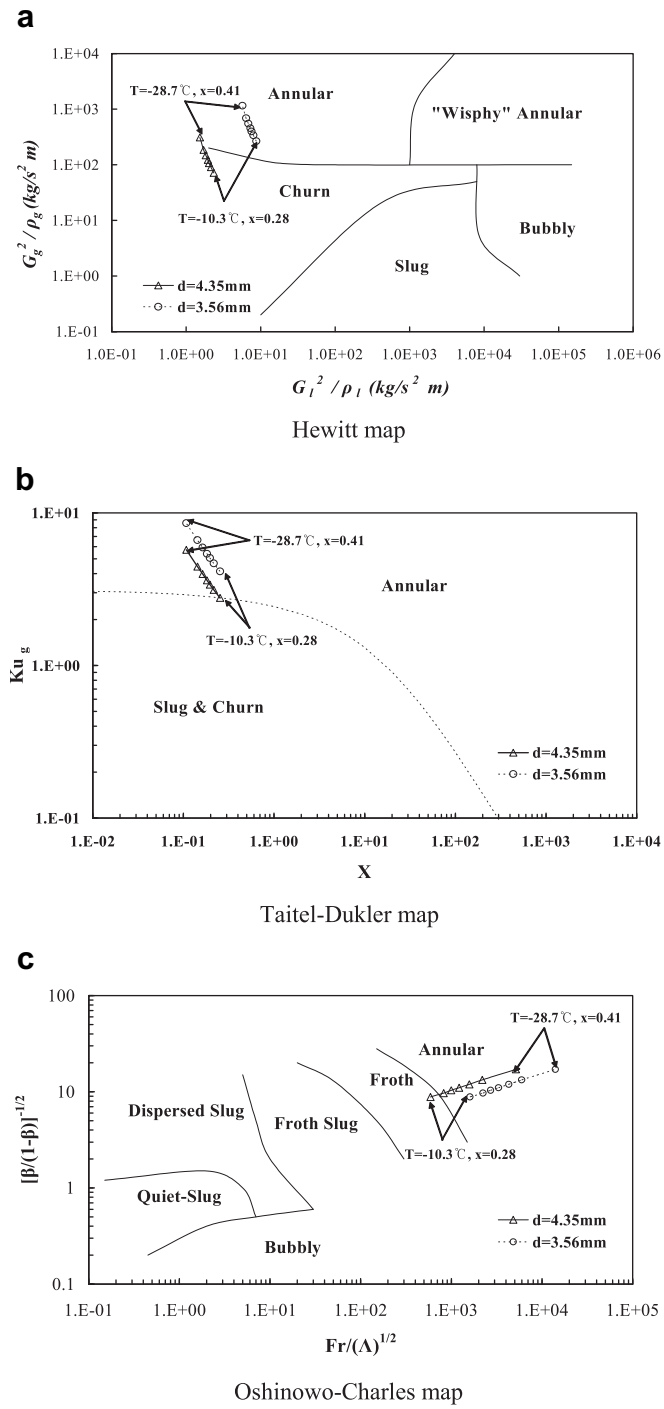

Fig. 6 – Estimation of the flow patterns at the evaporator-inlet pipe for the operating cycle of the commercial refrigerator according to the various diameter of the pipe.

When the amount of the gas increases in a 2-phase fluid of low velocity, a liquid bridge occurs in the 2-phase fluid and large bubbles can be produced. However, when the gas velocity is sufficiently fast, the liquid is swept up to the wall of the pipe and the liquid flows like the shape of the film on the wall side. Based on these theoretical considerations, the mass velocity (mass flux) of the gas becomes one of the main parameters defining the flow pattern in a pipe. The mass velocity is designed using the flow pattern map of vertical flow to prevent intermittent flow. The flow pattern maps considered in this section are the Hewitt map, Taitel–Dukler map and Oshinowo–Charles map.

In the Hewitt map, the parameters defining the flow pattern are mass velocity and density of the vapor and liquid. Based on the Hewitt map, the flow pattern is estimated to be annular flow when the mass velocity of the gas increases.

In the Taitel–Dukler map, the parameters defining the flow pattern are the Martinelli parameter and the Kutateladze

Table 5 – Estimation summaries of the flow patterns at the evaporator-inlet pipe for the operating cycle of the commercial refrigerator according to the various diameter of the pipe.

Operating time from start (min)		4	8	12	20	30	60	100
Temperature (°C)		−10.3	−11.3	−12.5	−14.6	−16.4	−19.5	−28.7
Pressure (Mpa)		0.1066	0.1026	0.09783	0.08995	0.08354	0.07361	0.04908
Vapor quality		0.28	0.31	0.33	0.34	0.36	0.38	0.41
Inner diameter of the pipe (mm)	Kind of flow pattern map	Estimated flow pattern						
$d_{in} = 5.6$	Hewitt map	C	C	C	C	C	C	C
	Oshinowo–Charles map	C	C	C	C	C	A	A
	Taitel–Dukler map	S/C	S/C	S/C	S/C	S/C	S/C	A
$d_{in} = 4.35$	Hewitt map	C	C	C	C	C	C	A
	Oshinowo–Charles map	C	A	A	A	A	A	A
	Taitel–Dukler map	S/C	A	A	A	A	A	A
$d_{in} = 3.56$	Hewitt map	A	A	A	A	A	A	A
	Oshinowo–Charles map	A	A	A	A	A	A	A
	Taitel-Dukler map	A	A	A	A	A	A	A

A: Annular, C: Churn, S: Slug, W: Wavy.

parameter of the gas as given in Table 3. Based on the Taitel–Dukler map, the flow pattern is estimated to be annular flow when the Martinelli parameter is low value and the Kutateladze parameter is high value. When the mass quality increases, the Martinelli parameter decreases. When the superficial velocity of the gas increases, the Kutateladze parameter also increases. Therefore, to produce annular flow in a pipe, the mass quality and velocity of the gas should be increased.

In the Oshinowo–Charles map, the parameters defining the flow pattern are volumetric quality and Froude number, as given in Table 3. Based on the Oshinowo–Charles map, the flow pattern transitions from churn to annular flow as the volumetric quality of the gas and Froude number increase. The Froude number increases when the superficial velocity is high and the diameter of the pipe is small. Therefore, to produce annular flow in a pipe, the superficial velocity should be increased and the diameter of the pipe should be reduced; this means that the mass velocity of the gas should be increased.

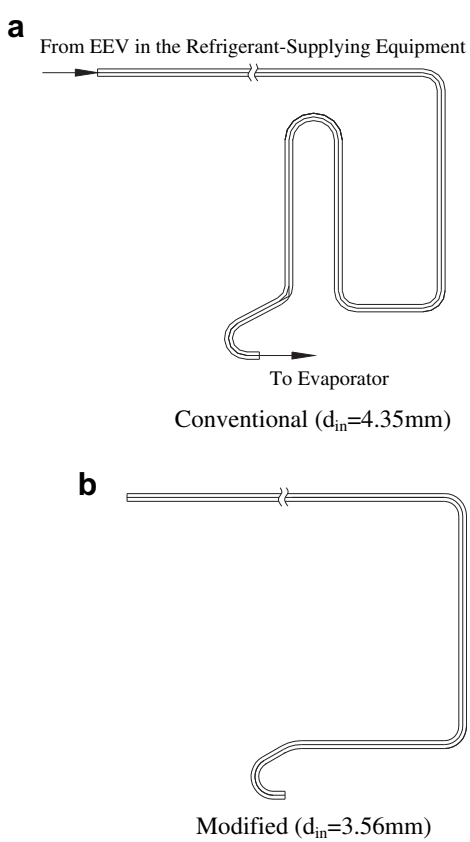

Fig. 7 – Modified design of the evaporator-inlet pipe for the test unit.

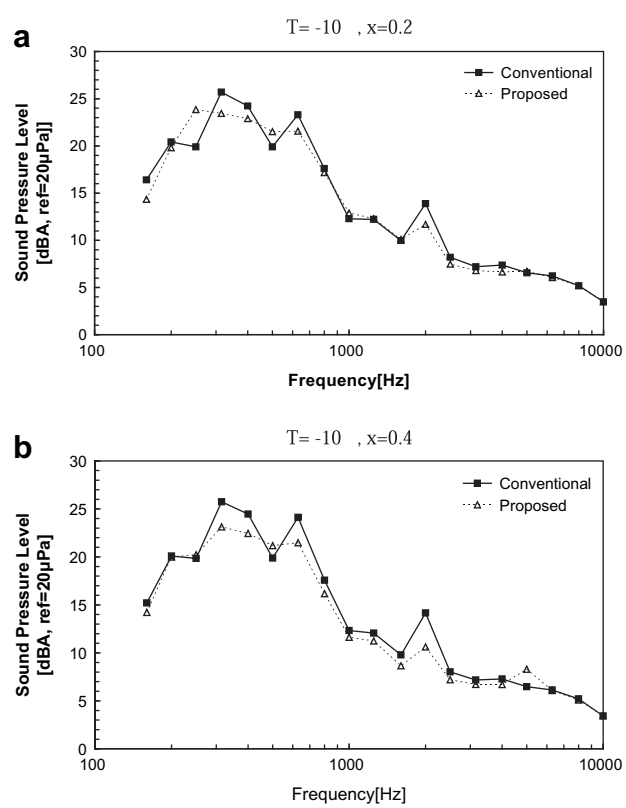

Fig. 8 – Comparison of 1/3 octave acoustic spectra at the evaporator-inlet pipe.

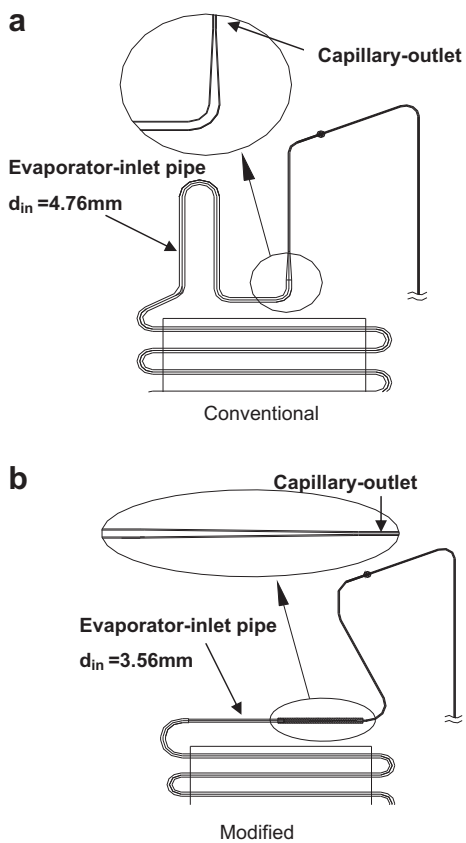

Fig. 9 – Modified design of the evaporator-inlet pipe for the refrigerator.

Based on the estimations of the flow pattern in the evaporator-inlet pipe with various flow pattern maps, the mass velocity should be increased in the evaporator-inlet to produce an annular flow pattern. In order to increase the mass velocity, the diameter of the pipe should be reduced. Fig. 6 and Table 5 show the flow patterns according to the different pipe diameters estimated from the Hewitt, Taitel–Dukler and Oshinowo–Charles flow pattern maps. In these flow patterns maps, the mass flow rate is 2.77 kg/h ± 1%. These estimations of the flow pattern show that the flow pattern becomes annular flow in the low vapor quality region of the refrigerator

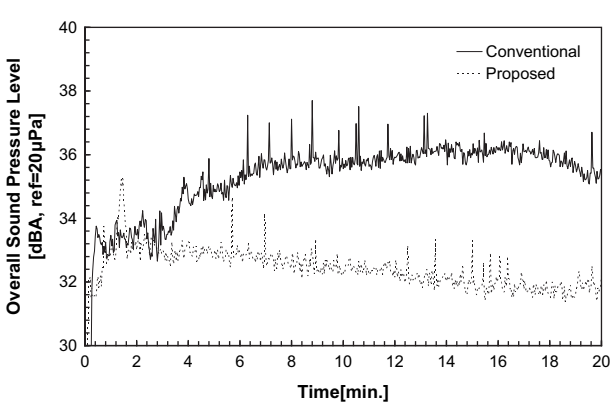

Fig. 10 – Overall sound pressure level of the refrigerator for 20 min from starting.

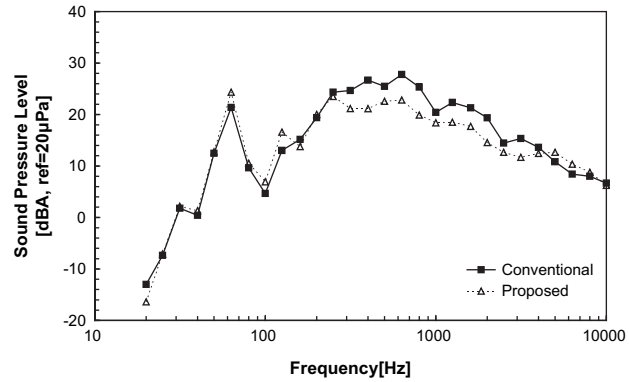

Fig. 11 – Comparison of 1/3 octave spectra of the refrigerator.

by reducing the diameter of the pipe. As referred in the previous chapter, the refrigerant-induced noise rarely occurs when the flow pattern in a pipe is annular. Therefore, it can be estimated that the refrigerant-induced noise could be reduced when the flow pattern transitioned from the churn (or slug) to the annular flow.

6. Validation

6.1. *Validation in test equipment*

In order to validate the noise reduction by transitioning of the flow pattern from intermittent to annular flow, an evaporator sample was manufactured as shown in Fig. 7 and a noise test was performed with the evaluation system. As shown in Fig. 7, a modified design is applied so that the unnecessary vertical pipe is removed and inner diameter of the evaporator-inlet pipe is reduced from 4.35 mm to 3.56 mm.

Fig. 8 shows the comparison of the acoustic spectra obtained from test between the conventional and the modified evaporator-inlet pipe when the vapor quality was 0.2 and 0.4. The temperature of the evaporator was −10 °C ± 1 °C and the mass flow rate was 2.77 kg/h ± 1%. Based on the estimation results of the flow pattern in the previous chapter, it can be known that the flow pattern may be slug or churn flow when $d = 4.35$ mm and be annular one when $d = 3.56$ mm. It denotes that the refrigerant-induced noise should be reduced when the diameter of the evaporator-inlet pipe is reduced from 4.35 to 3.56 mm due to the transition of the flow pattern.

From Fig. 8, the noise can be reduced by about 2–5 dB (31%–63% of the original sound pressure) at the frequency range of 315–400 Hz and by 3–5 dB (31%–50% of the original sound pressure) at 2 kHz when the evaporator-inlet pipe is modified, as shown in Fig. 7b.

6.2. *Validation in a real refrigerator*

In order to validate the results from the evaluation system of the refrigerant-induced noise, the evaporator assembly was redesigned, as shown in Fig. 9, and applied to a commercial

refrigerator. The inner diameter of the evaporator-inlet pipe was reduced from 4.35 to 3.56 mm and the direction of the pipe was laid horizontally. In addition, the direction of the capillary-outlet was modified from vertical to horizontal because the layout of the horizontal direction was considered to be better than that of the vertical one considering the relationship between flow pattern and refrigerant-induced noise.

Fig. 10 shows the comparison of the overall sound pressure level of the refrigerator between the conventional and modified model of the evaporator-inlet pipe. It was measured for 20 min from the start of operation of the compressor, at which moment the refrigerant-induced noise occurs most seriously in the refrigerator. The overall sound pressure level was reduced by a maximum of 4 dB (40% of the original sound pressure) when the modified evaporator-inlet pipe was applied. These results show good coincidence with the results from the test equipment in the previous section.

Fig. 11 shows the comparison of the 1/3 octave-band spectra for the noise between the conventional and the modified evaporator-inlet pipe. The noise level was reduced by about 2–5 dB (31%–63% of the original sound pressure) at the frequency range from 315 Hz to 3.15 kHz applying the modified evaporator-inlet pipe.

With these test data, it can be verified that the refrigerant-induced noise can be reduced when the flow pattern in a pipe is not intermittent flow but steady flow such as annular. The pipe should be better to be laid horizontally in order to prohibit the intermittent flow at operating condition of the refrigerator.

7. Conclusion

The refrigerant-induced noise of the refrigerator was strongly related to the flow pattern in a pipe. By theoretical review and tests with the evaluation system of refrigerant-induced noise, the relationship between refrigerant-induced noise and flow pattern in a pipe was found as below.

(1) Through the evaluation system, refrigerant-induced noise was increased when the flow pattern in the evaporator-inlet pipe was intermittent flow (churn flow), and reduced when the flow pattern transitioned from churn to annular flow.
(2) Through the estimations of the flow pattern by using horizontal and vertical flow pattern maps, the flow pattern in the vertical pipe was more likely to be intermittent flow rather than that of the horizontal one. Therefore, when the layout of the evaporator-inlet pipe was horizontal, refrigerant-induced noise was much less than when the layout of the evaporator-inlet pipe was vertical.
(3) In order to reduce refrigerant-induced noise from intermittent flow, mass velocity should be considered. The mass velocity of the gas should be made sufficiently fast to mitigate intermittent flow in a pipe.
(4) Removing unnecessary vertical pipes and adjusting the diameter of the evaporator-inlet pipe, the flow pattern in an evaporator-inlet pipe can be made to be annular flow. Refrigerant-induced noise in a refrigerator was reduced by about 2–5 dB at the frequency range from 315 Hz to 3.15 kHz, as validated by experiment in the test equipment and in a real refrigerator.

REFERENCES

Baker, O., 1954. Design of pipe lines for simultaneous flow of oil and gas. Oil Gas J. 53, 185–190.
Diatschenco, V., Brown, W.K., Stoy, J.R., 1994. Passive Acoustic Detection of Flow Regime in a Multi-phase Fluid Flow. United States Patent, Patent number: 5,353,627.
Han, H.S., Jeong, W.B., Kim, M.S., Kim, T.H., 2009. Analysis of the root causes of refrigerant-induced noise in refrigerators. J. Mech. Sci. Techn. 23, 3245–3256.
Hashizume, K., 1983. Flow pattern and void fraction of refrigerant two-phase flow in a horizontal tube. Bulletin of the JSME 26, 1597–1602.
Hewitt, G.F., Roberts, D.N., 1969. Studies of Two-phase Flow Patterns by Simultaneous Flash and X-ray Photography. Atomic Energy Research Establishment. Report No. AERE-M2159.
Mandhane, J.M., Gregory, G.A., Aziz, K., 1974. A flow pattern map for gas–liquid flow in horizontal pipes. Int. J. Multiphas. Flow 1, 537–553.
Minnaert, W.K., 1933. On musical air bubbles and the sound of running water. Phil. Mag. 16, 235–248.
Oguz, H.N., Prosperetti, A., 1998. The natural frequency of oscillation of gas bubbles in tubes. J. Acoust. Soc. Am. 103, 3301–3308.
Oshinowo, T., Charles, M.E., 1974. Vertical two-phase flow; Part1: flow pattern correlations. Can. J. Chem. Eng. 52, 25–35.
Strasberg, M., 1956. Gas bubbles as source of sound in liquids. J. Acoust. Soc. Am. 28, 20–27.
Taitel, Y., Dukler, A.E., 1976. A model for predicting flow regime transitions in horizontal and near horizontal gas–liquid flow. AIChE J. 22, 47–55.
Taitel, Y., Dukler, A.E., 1977. Flow regime transitions for vertical upward gas–liquid flow: a preliminary approach through physical modeling. In: AIChE 10th Annual Meeting, New York. Session on Fundamental Research in Fluid Mechanics.
Thome, J.R., Hajal, J.E., 2003. Two-phase flow pattern map for evaporation in horizontal tube: latest version. Heat Tran. Eng. 24, 3–10.